



Odd-Even Pattern Observed in Polyaniline/(Au₀ – Au₈) Composites

Alex P. Jonke,* Mira Josowicz,** and Jiří Janata**,*^z

School of Chemistry and Biochemistry, Georgia Institute of Technology, Atlanta, Georgia 30332, USA

Theoretically predicted effect of odd-even pattern of electron pairing on behavior of gold clusters in polyaniline/Au_N (N = 0 to 8) has been confirmed experimentally. In these composites the atomic Au clusters with even number of atoms exhibit higher catalytic activity for electrochemical oxidation of n-propanol in 1 M NaOH than the odd-number atoms clusters. Also, infrared spectroscopy shows that even numbered PANI/Au_N composites affect the N-H stretching vibration more strongly than the corresponding odd numbered ones. This behavior matches the theoretically predicted variations of HOMO-LUMO gap energy and the stability of the atomic Au clusters. It also agrees with the earlier experimental work in which the UPS spectra of isolated, mass-selected Au clusters have been reported.

© 2012 The Electrochemical Society. [DOI: 10.1149/2.053203jes] All rights reserved.

Manuscript submitted October 18, 2011; revised manuscript received December 1, 2011. Published January 12, 2012.

Nano-sized gold has been extensively investigated because physical and chemical properties of gold clusters are known to change with their size.^{1–3} Both bulk gold and gold nanoclusters have catalytic properties for oxidation of alcohols in alkaline medium,^{4–10} and for carbon monoxide.^{11,12} There are several reports of gold clusters containing only a few atoms being catalytically active.^{13,14} It has been predicted that the stability of atomic gold clusters of Au_N where N = 1–10 would depend on binding energy, dissociation energy, second order difference in total energy, and HOMO-LUMO energy gap.^{15–17} These theoretical studies shown that neutral (ground state) gold clusters exhibit an odd-even oscillation of their properties due to electron-pairing effect for the second order difference in total energy and in the HOMO-LUMO energy gap. Gold clusters made of 2 and 6 atoms have the largest HOMO-LUMO gap and dissociation energy, while the second order difference in total energy is the lowest for these two, which confirms their high stability.^{15–17} The even numbered gold clusters are more stable than the odd numbered clusters. Moreover the Au₂ and Au₆ clusters have two dimensional structures.^{18,19} The odd-even pattern of electronic properties of gold and other coinage metals, has been confirmed in the experiment in which the UPS spectra of mass-selected metal clusters have been measured.²⁰ In those experiments the oscillating pattern ceases at N > 20 (for gold) and the electron affinity assumes the value corresponding to bulk metal.

It is known that catalytic performances of gold clusters depend on their preparation methods, support matrix, and their size.^{13,21–26} In this study we use as the support matrix polyaniline (PANI) deposited on a Pt electrode. It has been demonstrated that both, PANI containing metal precipitates and PANI modified electrodes, show electrocatalytic oxidation of primary alcohols in alkaline and acidic medium,^{27–31} but the catalytic effect is higher in the alkaline medium. Polyaniline is highly stable and easy to prepare, and its properties have been extensively studied.^{32–34}

Here we report on the properties of PANI/Au_N composites made with N = 0 to 8 numbers of gold atoms. The composite has been prepared by a cyclic insertion of atom-by-atom of gold into PANI, by continuously controlling the oxidation potential of PANI and the exchange of the precursor medium throughout the gold insertion cycle.³⁵ Maintaining the PANI in high oxidation state was necessary in order to avoid spontaneous reduction of AuCl₄[–] to gold by the emeraldine form of PANI.^{36,37}

To show that the gold atoms deposited are not just many single atoms, but clusters of Au_N for N = 0 to 8, in this work we use the oxidation of n-propanol (n-PrOH) on gold as a marker to confirm the odd-even behavior of the clusters. The atomic gold clusters are assumed to reside in the vicinity of nitrogen sites in the PANI chain and should affect the N-H stretching frequencies in the IR spectrum

according to their size. The FTIR spectra obtained in this study further confirm the theoretically predicted odd-even pattern of behavior of these materials.

The oxidation of n-propanol in alkaline medium show very low activity on Pt electrode.³⁸ In contrast, gold shows high oxidation activity in alkaline solution because it is relatively immune to surface poisoning caused by side products of the primary alcohol oxidation.^{4,10} Furthermore, it has been shown that bulk Au as well as gold clusters of 2 to 5 nm supported on inorganic oxides or active carbon are highly active, selective, and recyclable catalyst for the oxidation of alcohols into aldehydes and ketones using oxygen at atmospheric pressure as the oxidant in the absence of solvent and base.^{39,40} Unusual electrocatalytic activity was observed for oxidation of methanol on gold nanoparticles in alkaline media synthesized in water-in-oil microemulsions using a rotating disk electrode.⁷

For the catalytic oxidation of n-propanol in alkaline solutions, the mechanism has been explained by the OH[–] anion adsorption onto the gold. The oxidation of the alcohol then occurs through hydrogen bridges formed between the hydroxyl group of the alcohol and the adsorbed anions.⁸ Although oxidation currents are much higher on bulk electrodes, the voltammetric characteristics are similar in both cases. Here we demonstrate that careful design of the atomic gold nanoparticles may affect significantly the alcohol oxidation process.

Experimental

Chemicals.— Tetrafluoroboric acid (HBF₄; Aldrich, 48 wt % solution in water), potassium tetrachloroaurate (KAuCl₄; Aldrich, 99.9%), aniline (C₆H₅NH₂; Aldrich, 99.51%), perchloric acid (HClO₄; EMD, 67–71%), n-propanol (C₃H₇OH; Aldrich, 99.5%), sodium hydroxide (NaOH; BDH), and hydrochloric acid (HCl; BDH, 38.0%) were all used as received.

Electrochemical preparation of polyaniline gold composite films.— The preparation of the PANI/Au_N films, where N equals the number of gold deposition cycles, was described previously.²⁰ Briefly, the PANI was deposited on one side of a Pt (1000 Å) coated on Ti (100 Å) 10 MHz polished quartz crystal (QC) (International Crystal Manufacturing OKC, OK, USA) from a 0.1 M aniline/2 M HBF₄ aqueous solution at a constant potential of +0.9 V for 200 seconds in a flow through cell. The flow through cell housing the Electrochemical Quartz Crystal Microbalance (EQCM) arranged in a flow injection analysis (FIA) format allows exchange of solutions while maintaining the electrical contact to the PANI film throughout the preparation steps of a deposition cycle. All potentials are referenced to the Ag/AgCl in 0.1 M KCl. The counter electrode was bare Pt deposited on quartz crystal. The electrochemically active area (A = 0.236 cm²) on the crystal was defined by the o-ring. Cyclic voltammograms (CV) were recorded with an Omni 90 potentiostat (Cypress Systems Lawrence, KS) and the changes of mass were obtained from the Sauerbrey

* Electrochemical Society Student Member.

** Electrochemical Society Active Member.

^z E-mail: jiri.janata@chemistry.gatech.edu

equation, using a PLO-10i phase lock oscillator (Maxtek, Inc. Cypress, CA) and a model 53131 A Universal Counter (Hewlett Packard Loveland, Co). All CVs were recorded with 20 mV/s scan rate. After coating the Pt electrode with PANI, the cell was rinsed with 0.1 M HCl, and the electrode was conditioned first by applying 10 CVs from -0.2 V to $+0.7$ V and then holding the potential at $+0.8$ V for 1 hour in this electrolyte.⁴¹ The average thickness of the PANI film prepared in this way was $4 \mu\text{m}$, as determined by the contact profilometry, and the average mass of the deposited PANI was 43 nmoles. After the conditioning step the flow cell was rinsed with a 0.1 M HClO_4 , and total of 10 CVs were completed from -0.2 V to $+0.7$ V. The Au-cycle was initiated by holding the PANI at $+0.7$ V while exposing it to solution of 10^{-4} M KAuCl_4 in 0.1 M HClO_4 for 50 seconds. Maintaining this high potential, keeps PANI in a fully oxidized state and leads to formation of the $\text{PANI}^+\text{AuCl}_4^-$ complex. The film was then rinsed of the excess of AuCl_4^- with 0.1 M HClO_4 , and the potential was scanned to -0.2 V in order to reduce AuCl_4^- to atomic gold. The total holding time at $+0.7$ V during the exposure to the chloroaurate solution and subsequent rinsing was 300 seconds. The final step was to perform 5 more CVs from -0.2 V to $+0.7$ V in order to bring the film to its defined final state. At this point, the material was ready for the next gold deposition cycle. The cycle was repeated N-times in order to form the PANI/Au_N of the desired composition. The N deposition cycles were varied from $N = 0$ to 8. CVs for the electro-oxidation of n-PrOH were recorded in 1 M NaOH at a scan rate of 20 mV/s from -0.6 V to $+0.45$ V using a Solartron SI1287 electrochemical interface. The reference electrode was a Ag/AgCl in 1 M KCl, and the counter electrode was a platinum foil.

Fourier Transform Infrared Spectroscopy (FTIR).— FTIR measurements were performed with a BIO-RAD FTS-6000 with a BIO-RAD UMA-500 IR microscope attachment in the range of 700–4000 wavenumbers. IR reflectance spectra were obtained using the rapid scan mode at the mirror modulation frequency of 20 kHz, with the aperture open, filter setting of 5, and resolution setting of 4 cm^{-1} . An average of 32 scans was used to produce each spectrum. The PANI samples were analyzed while still on the Pt QCM. Background spectra were obtained using the bare Pt surface on the QCM under the same spectroscopic conditions as the samples. The background was subtracted from the sample spectra using BIO-RAD WIN-IR PRO software. Areas and peak assignments were obtained using the same software.

Results

Electro-oxidation of n-propanol.— Before conducting the oxidation of n-propanol using the PANI/Au_N composites, the CVs of the bare Pt electrode as well as of the PANI film deposited on Pt electrode ($\text{PANI}/\text{Au}_{N=0}$) was examined in 1 M NaOH, Figure 1A.

It can be seen that during the anodic sweep, the platinum surface is oxidized that gives rise to a cathodic reduction peak on the reverse scan. The surface oxide formation is shifting to more negative potential for the PANI coated Pt electrode when compared to the bare Pt electrode. Upon addition of 0.5 M n-PrOH to the 1 M NaOH, the cyclic voltammograms at the bare Pt-electrode and at the PANI-coated Pt electrode are changing, Figure 1B. At the Pt electrode a small oxidation peak at -0.10 V is seen causing a slight enhancement of the reduction peak when compared with voltammogram shown in Figure 1A. A similar result was reported by others.³⁸

The voltammogram taken on the Pt/PANI shows two distinct oxidation peaks, on the forward scan at -0.27 V and on the reverse scan at -0.44 V. The enhanced magnitude of the peak current on Pt/PANI indicates much higher catalytic activity to n-PrOH than at the bare Pt electrode. The inset in Figure 1 shows the CV of the catalytic oxidation of 0.5 M n-PrOH in 1 M NaOH on a bare polycrystalline gold electrode. The oxidation peak in the forward scan occurs at $+0.18$ V, and on the reverse scan at $+0.08$ V. The reduction current corresponds to the reduction of surface gold oxide, and it increases with increasing the positive potential limit.⁵

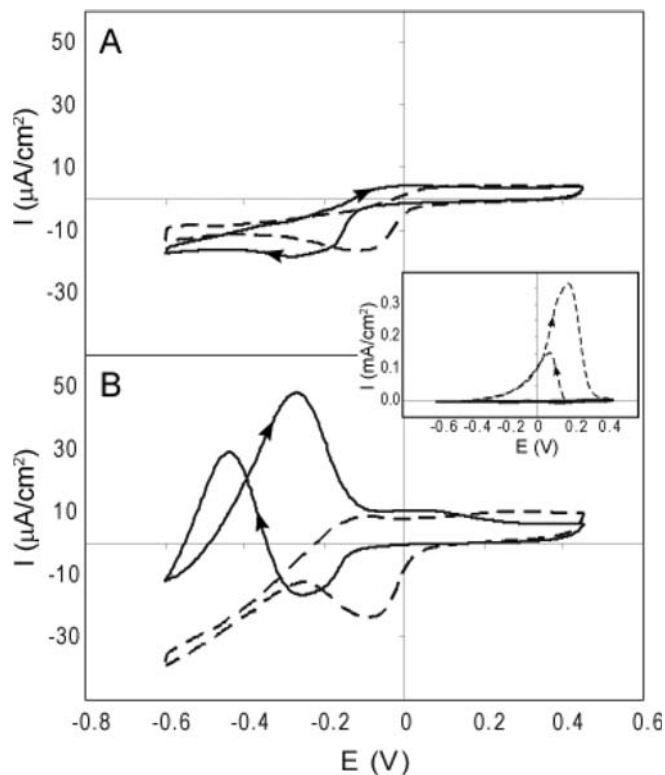


Figure 1. CVs of bare Pt (—) and PANI on Pt (---) in (A) 1 M NaOH and in (B) 0.5 M n-propanol in 1 M NaOH at 20 mV/s. Ten CVs were performed in the absence of n-propanol and five CVs were performed with n-propanol. Only the last CV for each is shown.

An overview of the effect of atomic gold in PANI on electrochemical oxidation of n-PrOH in alkaline medium is given in Fig. 2.

In this figure the CVs have been normalized to the mass of PANI deposited on the electrode in order to aid the visual comparison. The mass information is again obtained from the change of frequency of the EQCM during the deposition of the PANI, assuming the validity of the Sauerbrey equation in solution. For PANI/Au_0 , there is an oxidation peak in the forward scan around -0.27 V (peak I) and an oxidation peak in the reverse scan at -0.44 V, as seen previously in Fig. 1B, while voltammograms in the potential region above 0 V are featureless. On the other hand, in the $\text{PANI}/\text{Au}_{N>0}$ composites, a second oxidation peak (peak II) in the forward scan begins to emerge around $+0.12$ V, which is due to the oxidation of n-PrOH on the gold atomic clusters. It provides a strong indication that gold clusters are present in the films and that the presence of PANI provides a conducting network which facilitates the electrooxidation.

The peak II is shifted by -50 mV when compared with the oxidation peak potential on a polycrystalline gold electrode (see Fig. 1, Insert). It is important to point out that oxidation potential of peak (II) does not vary much with the number of Au atoms in the gold clusters; only the peak current is strongly affected. It suggests that the changes in peak current mirror the changes in the catalytic activity of n-PrOH oxidation (Figure 3).

It is observed, that by adding gold to the PANI films, the peak (I) also shows some oscillatory changes of the PANI activity in the presence of the alcohol, although less so than the peak (II) (Figure 3A). The highest catalytic activity is noticeable at 2 and 6 gold deposition cycles. The peak currents for the peak (II) in the forward scan are shown at the bottom of Figure 3. There is a substantial increase in peak current for PANI/Au_N where $N = 2, 4,$ and 6 , with $N = 6$ having the highest value. The fluctuation of the peak current density displays an odd-even pattern with the even numbered clusters showing the highest peak currents, with the exception of $N = 8$.

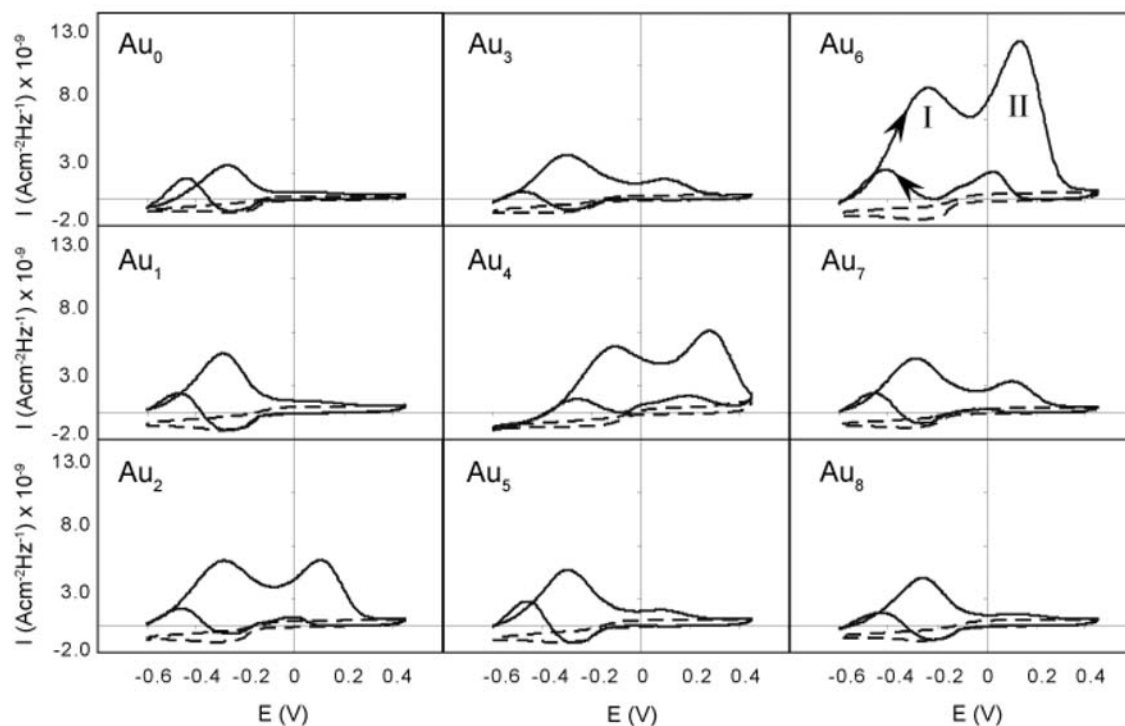


Figure 2. Effect of added 0 to 8 Au atoms to PANI on oxidation of 0.5 M n-propanol in 1 M NaOH (—) taken at 20 mV/s. The CVs in 1 M NaOH (---) are also shown. The CVs are normalized to the mass of PANI from the frequency changes during the deposition on Pt. Only the last CV of ten is shown in the absence of n-propanol, and only the last CV of five with n-propanol is shown for simplicity. The peaks (I) and (II) shown in PANI/Au₆ panel are discussed in the text.

Since catalysis only speeds up the rate of the reaction, the peak currents should increase linearly with concentration of the n-PrOH. The current densities for peaks (I) and peak (II) are plotted versus the concentration of n-propanol for PANI/Au₆ in Figure 4. The slopes

of the concentration dependence lines for peak (I) and peak (II) are $5.4 \times 10^{-8} \text{ mAcm}^{-2} \text{ M}^{-1}$, and $2.5 \times 10^{-7} \text{ mAcm}^{-2} \text{ M}^{-1}$, respectively.

FTIR of Au atoms in PANI.— It is expected that Au atoms will remain close to or at the nitrogen sites of PANI as they are formed in the polymer matrix. Consequently, the magnitude of the N-H stretching vibration in the region of 3100–3500 cm^{-1} should depend on the size and stabilities of the atomic Au clusters in the PANI. The FTIR spectra were recorded after cycling in 0.1 M HClO₄. Figure 5A shows the FTIR spectra for PANI/Au_N after N = 0 to 8 atomic gold cycles.

The presence of Au affects both the band position and the band intensity of the N-H stretch. The dependence of the band areas and the shifts of the band position from the Figure 5A are plotted in

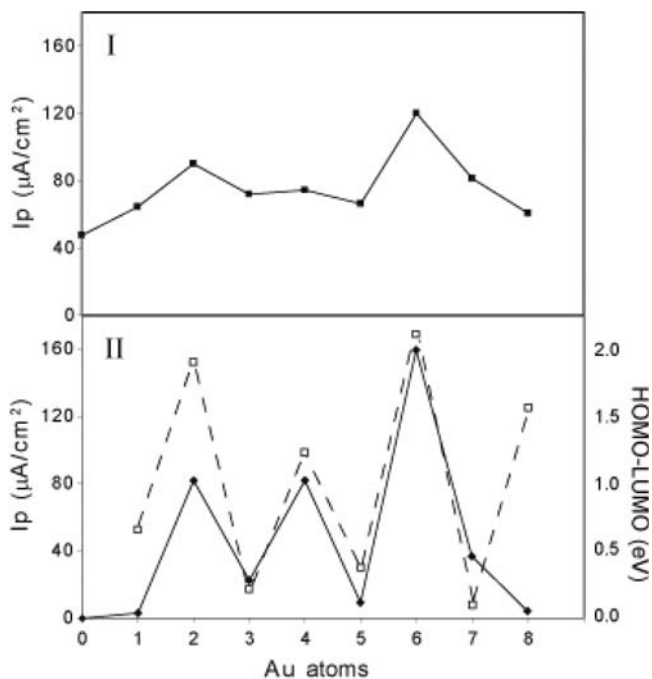


Figure 3. Peak current densities (evaluated from Figure 2) from the oxidation of n-PrOH versus the number of inserted gold atoms for (I) the first oxidation peak and (II) the second oxidation peak. Peaks I and II are labeled for Au₆ in Fig. 2. The concentration of n-PrOH was 0.5 M in 1 M NaOH. The dashed line represents calculated variation of the HOMO-LUMO gap energy^{15,16}

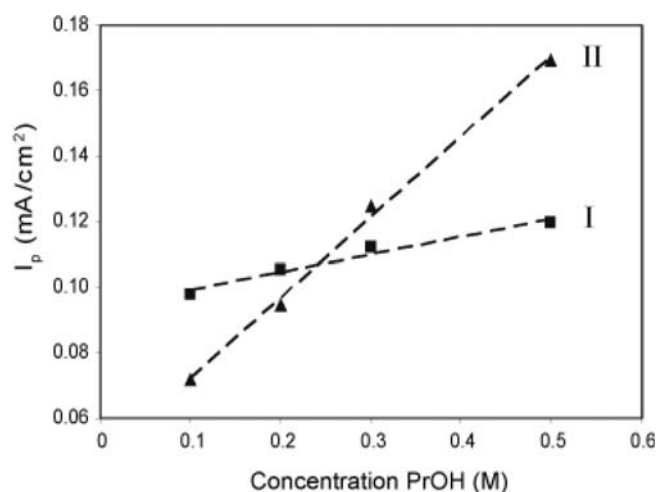


Figure 4. Linear dependence of peak current on n-PrOH concentration for PANI/Au₆ for (■) the first oxidation peak and (▲) second oxidation peak.

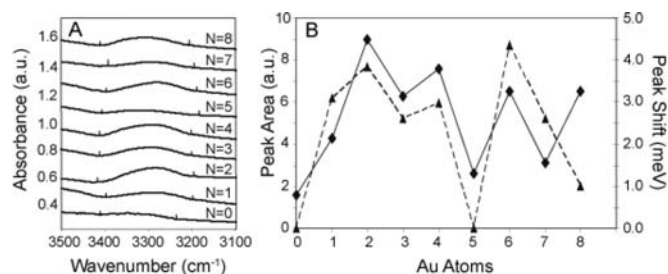


Figure 5. (A) FTIR spectra of PANI/Au_N for N = 0–8 from 3100–3500 cm⁻¹ showing the N-H stretching vibration. The marks on lines in (A) define the integration limits from which the peak areas were calculated. (B) FTIR peak areas (—◆—) and peak shifts (---▲---) of the peak for the N-H stretching at 3300 cm⁻¹ for PANI/Au_N for N = 0–8 showing an odd-even alternating pattern.

Figure 5B together with the number of gold cycles used for their accommodation in PANI. The band areas show an odd even pattern with the even number of atoms, yielding increased band areas relative to the odd number cluster of atoms. The band shifts also give an odd even pattern with the even number of atoms having a larger shift from the PANI/Au₀ than the odd number of atoms, with the exception of PANI/Au₈.

Conclusions

Electrooxidation of propanol in alkaline medium on Pt electrode is known to be significantly different from electrooxidation on Au. The difference is attributed to the presence of metal oxides. In this study we have shown that in addition to this material difference there is also a strong dependence on the number of gold atoms in atomic metal clusters. They showed catalytic activity for the oxidation of n-propanol which mirrors the theoretically predicted odd-even alternating pattern with the even number of atoms giving higher catalytic activity than the odd numbered atomic clusters. The most notable activity was obtained for the even numbers of N = 2, 4, and 6. It is expected that the oxidation of n-propanol leads to n-propanal and then to n-propionic acid as the final product.⁸

The band area and the band position for the N-H stretching vibration at 3300 cm⁻¹ in the PANI/Au composites are also perturbed by the presence of Au atoms. The odd-even alternation is again observed with the even numbered clusters affecting the N-H stretching vibration more strongly than the odd numbered clusters.

The confirmation of the odd-even oscillations for these clusters is significant in determining whether the Au atoms are deposited as individual atoms at different nitrogen sites in PANI, or if the atoms are deposited at the same site and form Au_N clusters. The observed odd-even oscillation pattern is a strong indication that these atoms are indeed atomic clusters of Au_N. However, this pattern breaks down for N = 8. A possible explanation for this deviation is that the clusters containing eight atoms of gold are so large that they do not fit into the confines of the PANI matrix and begin to bridge the distance between the neighboring clusters, allowing the clusters to aggregate. This explanation would be congruent with the model of Smalley²⁰ who prepared spatially unrestricted clusters. This point will be resolved by performing synchrotron radiation analysis of these materials.

Acknowledgment

Partial support of this project from the Georgia Research Alliance is greatly appreciated.

References

1. A. Sanchez, S. Abbet, U. Heiz, W. D. Schneider, H. Hakkinen, R. N. Barnett, and U. Landman, *J. Phys. Chem. A*, **103**, 9573 (1999).
2. A. S. K. Hashmi and G. J. Hutchings, *Angew. Chem. Int. Edit.*, **45**, 7896 (2006).
3. R. Meyer, C. Lemire, S. K. Shaikhutdinov, and H. Freund, *Gold Bull.*, **37**, 72 (2004).
4. K. A. Assiongbon and D. Roy, *Surf. Sci.*, **594**, 99–119 (2005).
5. Z. Borkowska, A. Tymosiak-Zielinska, and R. Nowakowski, *Electrochim. Acta*, **49**, 2613 (2004).
6. R. B. de Lima and H. Varela, *Gold Bull.*, **41**, 15–22, (2008).
7. J. Hernandez, J. Solla-Gullon, E. Herrero, A. Aldaz, and J. M. Feliu, *Electrochim. Acta*, **52**, 1662 (2006).
8. P. Ocon, C. Alonso, R. Celdran, and J. Gonzalezvelasco, *J. Electroanal. Chem.*, **206**, 179 (1986).
9. M. BeltowskaBrzezinska, T. Luczak, and R. Holze, *J. Appl. Electrochem.*, **27**, 999 (1997).
10. Y. Kwon, S. C. S. Lai, P. Rodriguez, and M. T. M. Koper, *J. Am. Chem. Soc.*, **133**, 6914.
11. Y. Iizuka, H. Fujiki, N. Yamauchi, T. Chijiwa, S. Arai, S. Tsubota, and M. Haruta, *Catal. Today*, **36**, 115 (1997).
12. B. K. Min and C. M. Friend, *Chem. Rev.*, **107**, 2709 (2007).
13. S. Lee, L. M. Molina, M. J. Lopez, J. A. Alonso, B. Hammer, B. Lee, S. Seifert, R. E. Winans, J. W. Elam, M. J. Pellin, and S. Vajda, *Angew. Chem. Int. Edit.*, **48**, 1467 (2009).
14. M. J. Rodriguez-Vazquez, M. C. Blanco, R. Lourido, C. Vazquez-Vazquez, E. Pastor, G. A. Planes, J. Rivas, and M. A. Lopez-Quintela, *Langmuir*, **24**, 12690 (2008).
15. E. M. Fernandez, J. M. Soler, I. L. Garzon, and L. C. Balbas, *Phys. Rev. B*, **70** (2004).
16. H. Hakkinen and U. Landman, *Phys. Rev. B*, **62**, R2287 (2000).
17. C. Majumder and S. K. Kulshreshtha, *Phys. Rev. B*, **73** (2006).
18. E. Janssens, H. Tanaka, S. Neukermans, R. E. Silverans, and P. Lievens, *New J. Phys.*, **5** (2003).
19. T. Risse, S. Shaikhutdinov, N. Nilius, M. Sterrer, and H. J. Freund, *Accounts Chem. Res.*, **41**, 949 (2008).
20. K. J. Taylor, C. L. Pettiettehall, O. Cheshnovsky, and R. E. Smalley, *J. Chem. Phys.*, **96**, 3319 (1992).
21. W. Eberhardt, *Surf. Sci.*, **500**, 242 (2002).
22. M. Haruta, *Catal. Today*, **36**, 153 (1997).
23. H. Miyamura, R. Matsubara, Y. Miyazaki, and S. Kobayashi, *Angew. Chem. Int. Edit.*, **46**, 4151 (2007).
24. L. Prati and M. Rossi, *J. Catal.*, **176**, 552 (1998).
25. D. Saio, T. Amaya, and T. Hirao, *Adv. Synth. Catal.*, **352**, 2177.
26. H. Tsunoyama, H. Sakurai, Y. Negishi, and T. Tsukuda, *J. Am. Chem. Soc.*, **127**, 9374 (2005).
27. K. L. Nagashree and M. F. Ahmed, *Synth. Met.*, **158**, 610 (2008).
28. K. L. Nagashree and M. F. Ahmed, *J. Appl. Electrochem.*, **39**, 403 (2009).
29. S. Palmero, A. Colina, E. Munoz, A. Heras, V. Ruiz, and J. Lopez-Palacios, *Electrochem. Commun.*, **11**, 122 (2009).
30. R. K. Pandey and V. Lakshminarayanan, *J. Phys. Chem. C*, **113**, 21596 (2009).
31. D. W. Hatchett, N. M. Millick, J. M. Kinyanjui, S. Pookpanratana, M. Bar, T. Hofmann, A. Luinetti, and C. Heske, *Electrochim. Acta*, **56**, 6060.
32. E. M. Genies, A. Boyle, M. Lapkowski, and C. Tsintavis, *Synth. Met.*, **36**, 139 (1990).
33. E. T. Kang, K. G. Neoh, and K. L. Tan, *Prog. Polym. Sci.*, **23**, 277 (1998).
34. A. A. Syed and M. K. Dinesan, *Talanta*, **38**, 815 (1991).
35. A. P. Jonke, M. Josowicz, J. Janata, and M. H. Engelhard, *J. Electrochem. Soc.*, **157**, P83 (2010).
36. D. W. Hatchett, M. Josowicz, J. Janata, and D. R. Baer, *Chem. Mater.*, **11**, 2989 (1999).
37. J. A. Smith, M. Josowicz, and J. Janata, *J. Electrochem. Soc.*, **150**, E384 (2003).
38. H. P. Liu, J. Q. Ye, C. W. Xu, S. P. Jiang, and Y. X. Tong, *J. Power Sources*, **177**, 67–70, (2008).
39. J. L. Gong, D. W. Flaherty, T. Yan, and C. B. Mullins, *Chemphyschem*, **9**, 2461 (2008).
40. A. Abad, P. Concepcion, A. Corma, and H. Garcia, *Angew. Chem. Int. Edit.*, **44**, 4066 (2005).
41. A. P. Jonke, M. Josowicz, and J. Janata, *J. Electrochem. Soc.*, **158**, E147 (2011).